Top-quark effects in $gg \to \gamma\gamma$ at NLO QCD

Xiaoran Zhao[1]

with Fabio Maltoni(UCLouvain&U. Bologna), Manoj K. Mandal(U. Padova)

Based on arXiv:1812.08703 and arXiv:19xx.xxxxx

[1]Centre for Cosmology, Particle Physics and Phenomenology (CP3)
Université catholique de Louvain, Belgium

September 12, 2019

The $\gamma\gamma$ channel

- Clean finalstate at LHC
- One main channel for Higgs discovery, and study Higgs properties
- Important channel for searching various kind of new physics, e.g.
  - New scalar or spin-2 resonance
  - Multiple resonances from extra-dimension/clockwork models
  - Peak-dip structures due to new particles in loops

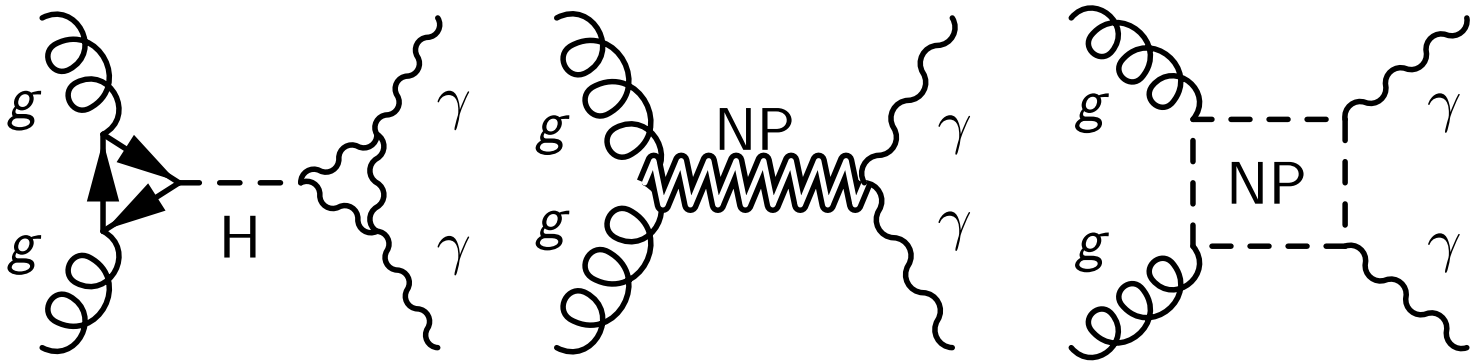

Theoretical status

- LO $q\bar{q} \to \gamma\gamma$
- NLO known since 2000 Binoth, Guillet, Pilon, Werlen'EPJC(16)311
- NNLO recently Catani, Cieri, deFlorian, Ferrera, Grazzini'PRL(108)072001, Campbell, Ellis, Li, Williams'JHEP(2016)07148 Grazzini, Kallweit, Wiesemann'EPJC(78)537

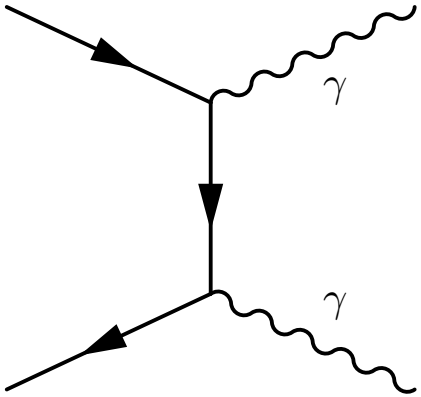

The loop-induced gluon fusion $gg \to \gamma\gamma$:

- Formally part of NNLO
- Anomalously large due to gluon-gluon luminosity.
- Separately gauge-invariant and IR finite.
- Can be treated as a standalone channel.

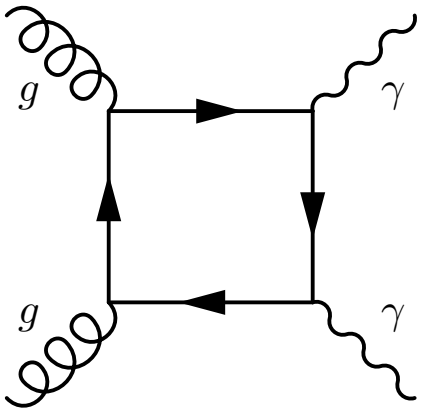

gluon fusion into diphoton: NLO status

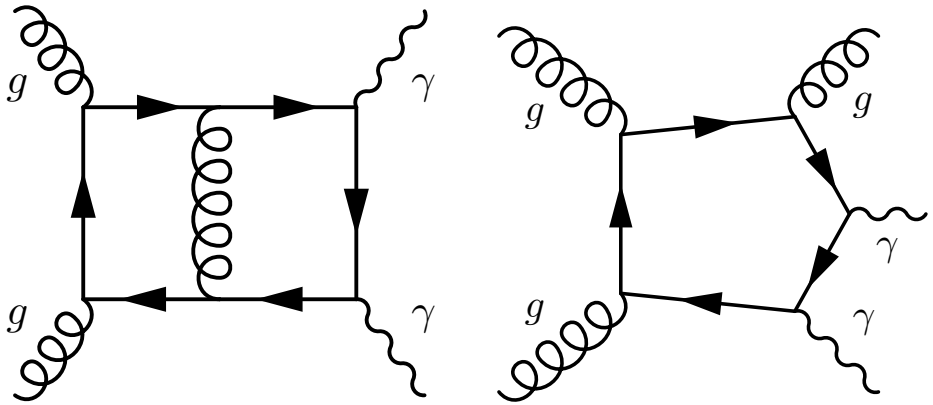

- Formally part of NNNLO corrections to $q\bar{q} \to \gamma\gamma$.
- NLO known for massless quarks only. Bern, Dixon, Schmidt'PRD66,074018

The top quark contribution is missing! How large could it be? Naively counting electric charge:

$$\frac{\sigma(6F)}{\sigma(5F)} = \frac{(\sum_{6F} Q_f^2)^2}{(\sum_{5F} Q_f^2)^2} \approx 1.86$$

Calculation framework

$$\mathrm{d}\sigma^{\mathrm{NLO}} = \mathrm{d}\sigma^{\mathrm{LO}} + \mathrm{d}\sigma^{\mathrm{V}} + \mathrm{d}\sigma^{\mathrm{R}} + \mathrm{d}\sigma^{\mathrm{C}}$$

- Madgraph5_aMC@NLO and Recola2 for $gg \to \gamma\gamma g$, $gq \to \gamma\gamma q$, $q\bar{q} \to \gamma\gamma g$ amplitudes Alwall, et.al'JHEP(2014)07079 Denner, Lang, Uccirati'CPC(224)346
- Dipole subtraction for IR divergences Catani, Seymour'NPB(485)291
- Main challenge: the two-loop virtual amplitude $gg \to \gamma\gamma$

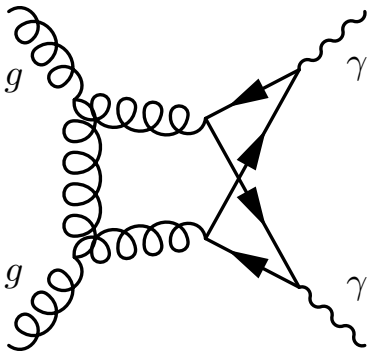

Massless case known since 2001 Bern, De Freitas, Dixon'JHEP(2001)09037

Massive case remains unknown, only some master integrals known analytically(mainly planar)

The two-loop massive amplitude

- 138 Diagrams generated via QGRAF
- Processed through FORM
- Projector methods: 10 projectors in D-dimension
- $\sim$40000 scalar integrals at 2-loop, distributed into 33 families
- IBP reduction performed by FIRE5 with LiteRed
- yield 1180 master integrals, not counting relations between families. (161 master integrals if symmetries are considered)

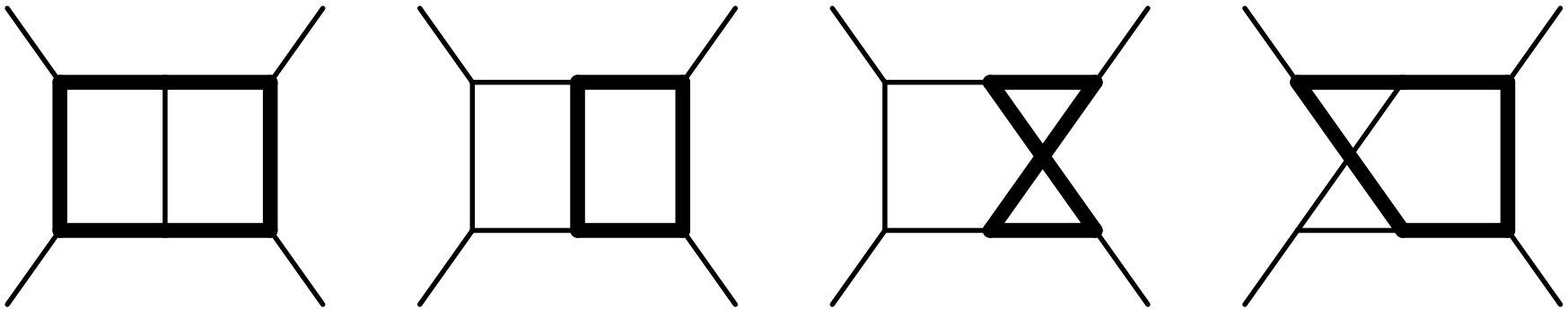

With integrate-by-parts(IBP) reduction, differential equations(DE) can be obtained:

$$I = \int \prod_{i=1}^{L} \mathrm{d}^d k_i \frac{1}{\prod_{j=1}^{N} D_j^{a_j}}$$

- iterative integration over all kinematics
- Numerical methods for Ordinary DE
- Initial value problem

$$\frac{\partial I(x;\epsilon)}{\partial x_i} = J_i(x;\epsilon) I(x;\epsilon)$$

[M.K. Mandal, XZ'JHEP(2019)03190]

- Initial condition obtained from the sector decomposition(SD) method
- Initial condition obtained in the unphysical region
- Analytically continuation to the physical region along integration contour

The initial condition

- The sector decomposition method: systematically resolve UV and IR divergence Binoth, Heinrich'NPB(585)741
- Integrand behaves good in Euclidean region
- Numerical integration: good convergence via quasi-Monte Carlo
- Implemented in NIFT

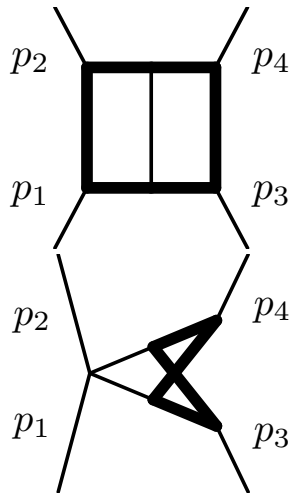

			c_0	time(s)
I_1	IC1	NIFT	−0.059087788(6)	1.93
		analytic	−0.059087788	–
	IC2	NIFT	−0.056016652(5)	1.74
		analytic	−0.056016650	–
I_2^{sub}	IC1	NIFT	0.28729542(1)	3.55
		analytic	0.28729543	–
	IC2	NIFT	0.26181028(1)	3.57
		analytic	0.26181029	–

IC1:$s = -1.33, t = -0.891$. IC2:$s = -1.3, t = -0.632$

Integration contour

- The contour should not cross branch cuts.

From $(s, t) = (-1.33, -0.891)$ to $(s, t) = (5, -2)$

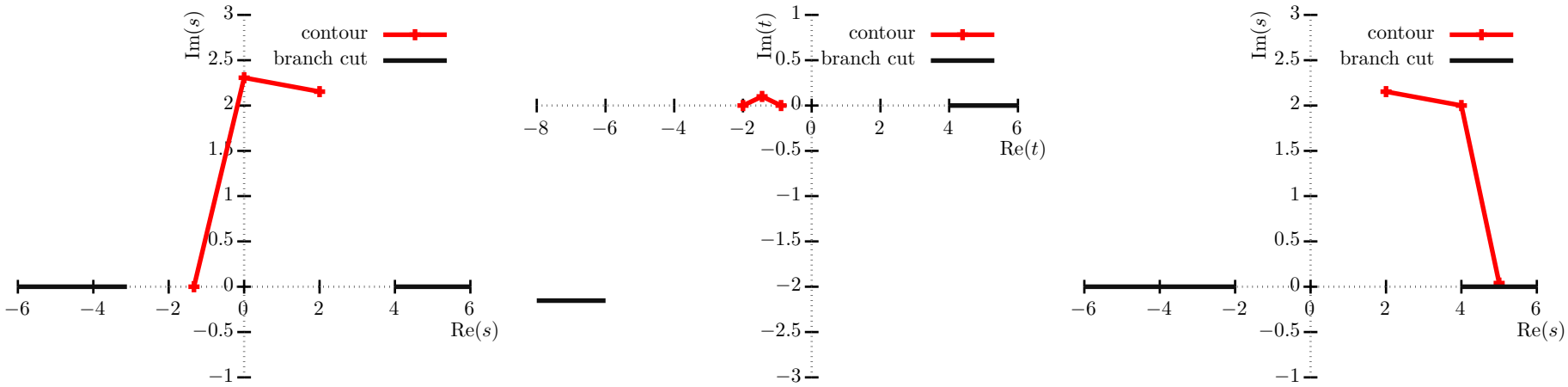

$(s=5, t=-2)$		c_0	time(s)
I_1	IC1	$0.573661717 - i0.45602298$	0.11
	IC2	$0.573662051 - i0.45602316$	0.10
	Analytic	$0.573661756 - i0.45602309$	–
I_2^{sub}	IC1	$-0.077764616 + i0.34306744$	0.26
	IC2	$-0.077764595 + i0.34306737$	0.23
	Analytic	$-0.077764620 + i0.34306741$	–

$(s=5, t=-2)$		c_0	c_1	c_2	time(s)
I_2	IC1	$0.02188084 - i0.00000002$	$-0.0870259 + i0.05170117$	$-0.246416 - i0.17602070$	0.26
	IC2	$0.02188080 + i0.00000001$	$-0.0870262 + i0.05170118$	$-0.246417 - i0.17602072$	0.23
	pySecDec	$0.02187(3) + i0.00003(3)$	$-0.0869(3) + i0.0518(4)$	$-0.248(2) - i0.175(2)$	$\mathcal{O}(10^4)$
I_3	IC1	$-0.0599222 + i0.4204527$	$-1.2093294 + i1.1271787$	$-3.737851 + i0.435880$	0.74
	IC2	$-0.0599219 + i0.4204528$	$-1.2093298 + i1.1271798$	$-3.737851 + i0.435879$	0.78
	pySecDec	$-0.05998(7) + i0.42048(8)$	$-1.2100(7) + i1.1262(7)$	$-3.737(3) + i0.430(3)$	$\mathcal{O}(10^4)$

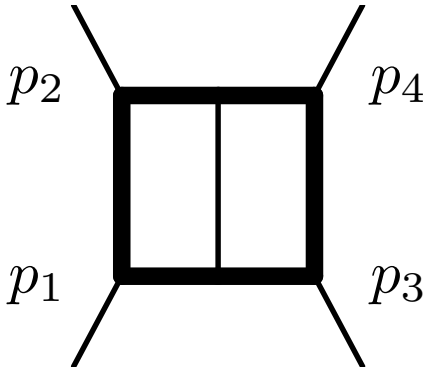

I_1

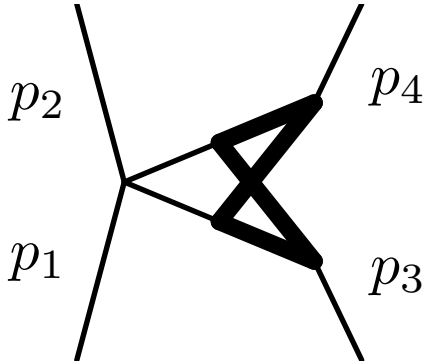

I_2^{sub}

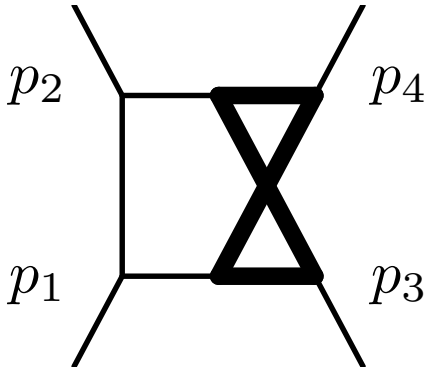

I_2

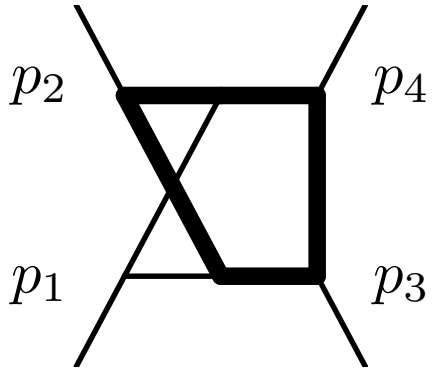

I_3

Initial condition tables

- Originally:

$$x_{SD} \xrightarrow{\text{long and complicated contour}} \{x_{target}\} \tag{1}$$

- Now:
  - Step 1: predefined set S_{tab} in the physical region

$$x_{SD} \xrightarrow{\text{long and complicated contour}} \{x | x \in S_{tab} \subset S_{phy}\} \tag{2}$$

    Storing the results at S_{tab}!
  - Step 2: pick one x_{tab} from S_{tab}!

$$x \in S_{tab} \xrightarrow{\text{short contour}} \{x_{target}\} \tag{3}$$

- Much($\mathcal{O}(10)$) less number of steps$\rightarrow$ $\mathcal{O}(10)$ times faster!
- Higher accuracy in the first step can be adopted.

Further optimization

- t is unchanged during s evolution! $\rightarrow$ Reorganizing the expressions so that the coefficients can be cached!

$$\frac{\partial I}{\partial s} = P_s(\{\epsilon, s, t\}; \mathbb{Z})I \rightarrow \frac{\partial I}{\partial s} = P_s(\{\epsilon, s\}; \mathcal{R}(\{t\}; \mathbb{Z}))I \tag{4}$$

$$\frac{\partial I}{\partial t} = P_t(\{\epsilon, s, t\}; \mathbb{Z})I \rightarrow \frac{\partial I}{\partial t} = P_t(\{\epsilon, t\}; \mathcal{R}(\{s\}; \mathbb{Z}))I \tag{5}$$

- Better numerical stability for backward region($|u| \ll |t|, |s|$): using u to compute the right-hand side

$$\frac{\partial I}{\partial s} = Q_s(\epsilon, u; \mathcal{R}(\{t\}; \mathbb{Z}))I \tag{6}$$

$$\frac{\partial I}{\partial t} = Q_t(\epsilon, u; \mathcal{R}(\{s\}; \mathbb{Z}))I \tag{7}$$

Overview of numerical code

- $\sim$ 10000 CPU hours to obtain initial conditions through numerical integration
- $\mathcal{O}(10^{-9})$ precision or higher for all MIs
- Up to $\mathcal{O}(\epsilon)$ for 7-prop MIs, $\mathcal{O}(\epsilon^2)$ for others.
- Amplitude evaluation costs $\sim$1 second per phasespace point!

Top quark only

Firstly we consider the case that only including the top quark contribution:

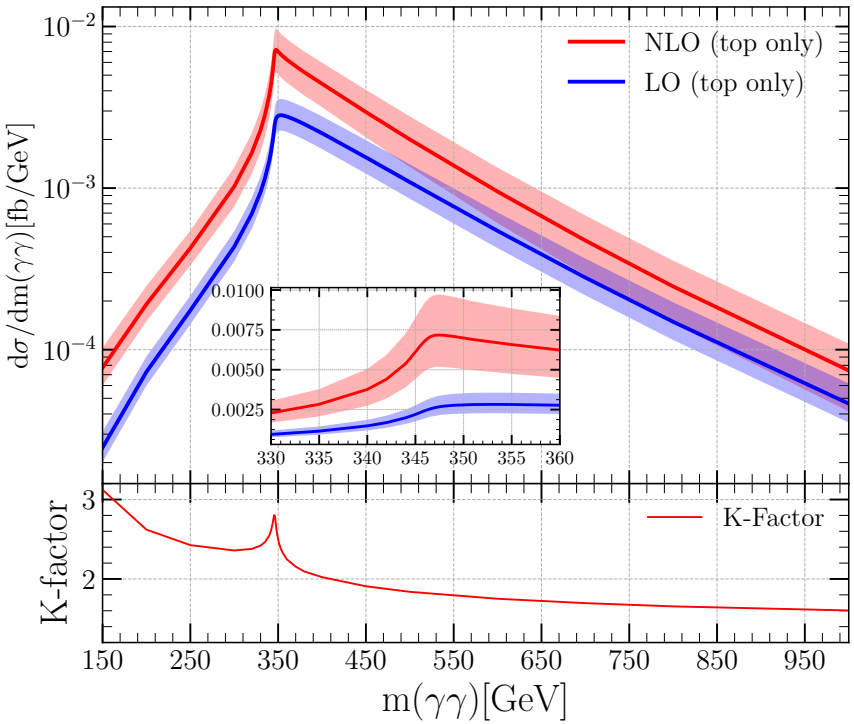

- Tiny cross section in low energy region,
- The cross section peaks around top pair threshold
- Huge NLO corrections, decrease as $m(\gamma\gamma)$ increases
- Threshold region enhanced due to Coulomb gluon effects.

Resumming Coulomb gluons

- Coulomb gluon exchange yields corrections as $\alpha_S/v \to$ spoil perturbativity
- One Coulomb gluon exchange: included in the two-loop amplitude
- Multiple Coulomb gluon exchange: formation of toponium $T(nS)$!

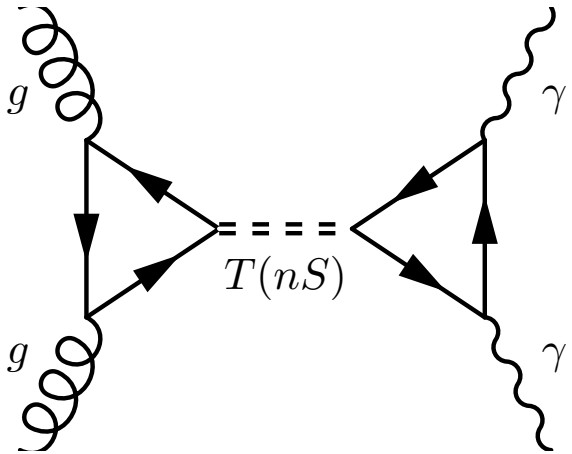

$$M^{2L} \to M^{2L,match} = M^{2L} + BG_{DT} \quad (8)$$

$$G_{DT} = \sum_{n=1}^{+\infty} -\frac{512 m_t^4}{27 n^3 \pi^5} \alpha_S^3 (\arcsin \frac{\sqrt{s}}{2m_t})^4 \frac{1}{s - m_n^2} \quad (9)$$

Coefficients can be determined by matching it to NRQCD predictions

Matched results

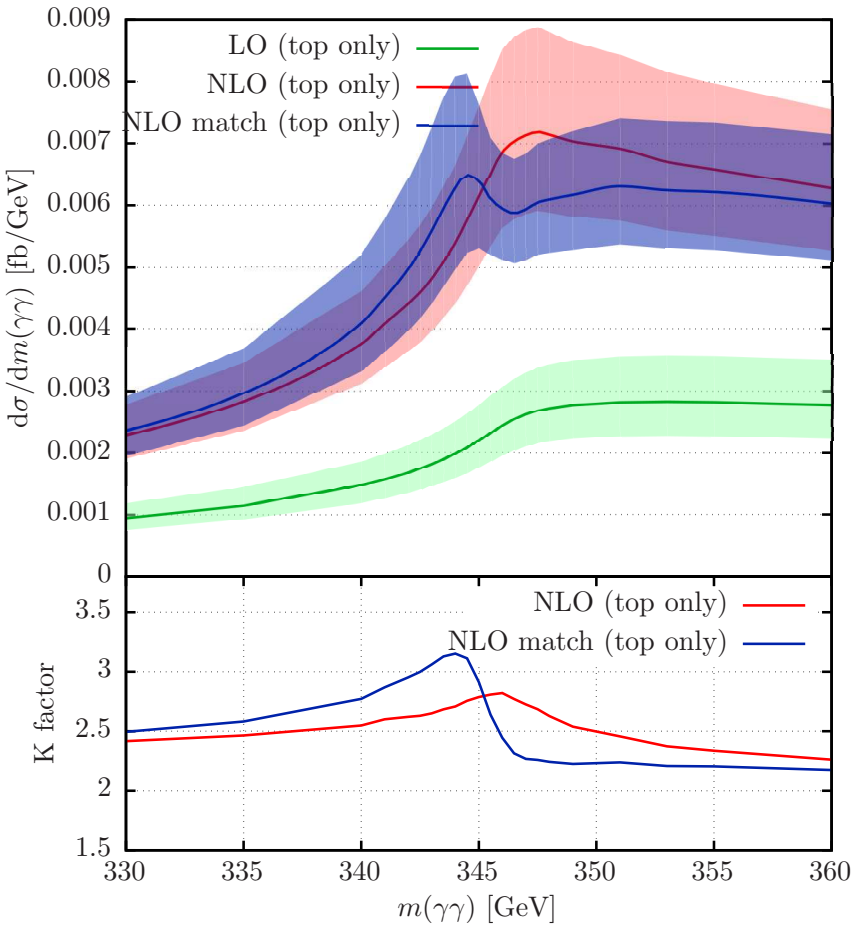

- Peak from Toponium($T(1S)$)
- Cancellation between one Coulomb gluon exchange and bound-states at $\sqrt{s} = 2m_t$.
- Bound-state contribution diminishes away from threshold

Low-energy behavior

Low energy$\rightarrow$ EFT. Only Abelian part now$\rightarrow$ QED.

$$\mathcal{L} = -\frac{1}{4}F^{\mu\nu}F_{\mu\nu} + \frac{\alpha^2 Q^4}{m^4}c_1(F^{\mu\nu}F_{\mu\nu})^2 + \frac{\alpha^2 Q^4}{m^4}c_2(\frac{1}{4}F^{\mu\nu}\epsilon_{\mu\nu\rho\lambda}F^{\rho\lambda})^2 \quad (10)$$

$$c_i = c_i^{1L} + \frac{\alpha Q^2}{4\pi}c_i^{2L} + \ldots, \quad i = 1, 2 \quad (11)$$

Numerical extrapolation $\rightarrow$Low precision!

Alternatively, we calculate the limit based on Cauchy integral formula:

$$f(s=0) = \frac{1}{2\pi i}\oint \mathrm{d}s\frac{f(s)}{s} = \int_0^{2\pi}\mathrm{d}\phi f(s = |r|e^{i\phi}) \quad (12)$$

	analytic(e.g. 1612.07251)	ours
c_1^{1L}	$\frac{1}{90} = 0.0111111111111\cdots$	0.011111111114(6)
c_2^{1L}	$\frac{7}{90} = 0.0777777777777\cdots$	0.07777777778(1)
c_1^{2L}	$\frac{16}{81} = 0.197530864\cdots$	0.1975308(1)
c_2^{2L}	$\frac{263}{162} = 1.623456790\cdots$	1.6234568(2)

Threshold behavior

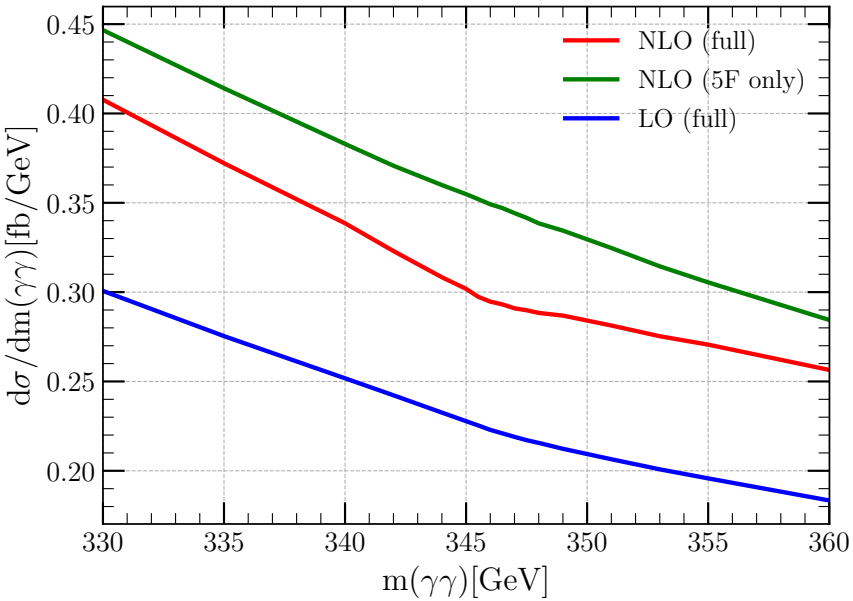

The threshold region

- Including the top quark decreases the cross section
- Slope changes more visible at NLO.
- Possibility of extracting the top quark mass here.

Differential cross section

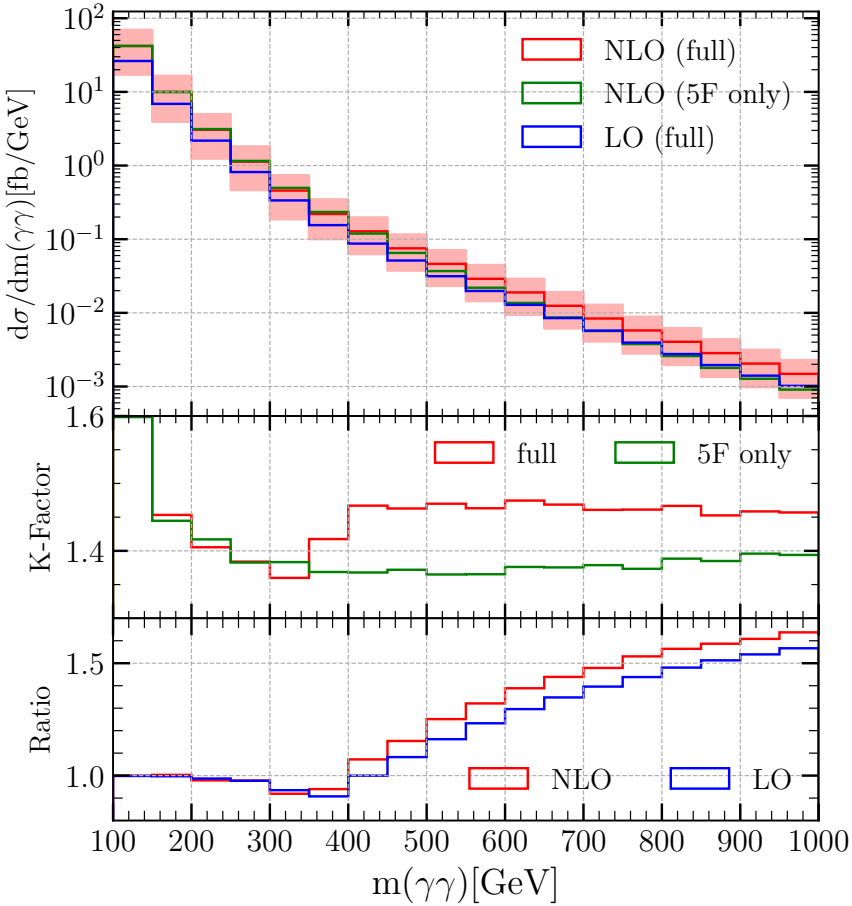

- Negligible effects below top pair threshold
- Decrease the cross section at the threshold region
- Larger K-factor above the threshold region.
- As $m(\gamma\gamma)$ increases, slowly approaching naive six-flavour limit(≈ 1.86)

Conclusion

- NLO corrections to $gg \to \gamma\gamma$
- Including both light quarks and the top quark
- Numerical methods for the two-loop massive amplitudes
- Large NLO corrections for the top quark contribution
- Coulomb gluon effects
- Low-energy behavior and Wilson coefficients
- More visible slope changes below and above top pair threshold
- Further enhancement beyond threshold region